ARTICLE

Oceanographic influences on patterns in North Pacific salmon abundance

Megan M. Stachura, Nathan J. Mantua, and Mark D. Scheuerell

Abstract: We identified three dominant patterns of temporal variation (1951–2002) in the abundance of 34 stock groups of wild North American and Asian pink salmon (*Oncorhynchus gorbuscha*), chum salmon (*Oncorhynchus keta*), and sockeye salmon (*Oncorhynchus nerka*) that were related to patterns of oceanographic variability. We identified these patterns using three different ordination methods and found consistent patterns across these methods. Alaskan salmon dominated the most prominent pattern, which exhibited a positive abundance shift in the mid-1970s. In general, warm (cold) periods in the Gulf of Alaska and eastern Bering Sea corresponded with high (low) abundance years for these stock groups. The second abundance pattern captured differences among Asian, northern North American, and southern North American population groups and was associated with an intense, large-scale Aleutian Low. To our knowledge, this is the first analysis that identifies regional patterns of covariation in salmon abundance around the entire North Pacific Rim, and it highlights the existence of basin-wide covariations in wild salmon abundance that are associated with spatially coherent and regionally distinct patterns in North Pacific climate.

Résumé : Nous avons établi l'existence de trois motifs prédominants de variation temporelle (1951–2002) de l'abondance de 34 groupes de stocks de saumons roses (*Oncorhynchus gorbuscha*), kéta (*Oncorhynchus keta*), et sockeye (*Oncorhynchus nerka*) sauvages nord-américains et asiatiques, associés à des motifs de variabilité océanographique. Pour ce faire, nous avons utilisé trois méthodes d'ordination distinctes et observé des motifs cohérents d'une méthode à l'autre. Le motif le plus évident, un changement positif de l'abondance au milieu des années 1970, était représenté en majeure partie par des saumons de l'Alaska. En général, les périodes chaudes (froides) dans le golfe d'Alaska et l'est de la mer de Behring correspondaient à des années de forte (faible) abondance pour ces groupes de stocks. Le deuxième motif d'abondance faisait ressortir des différences entre les groupes de populations de l'Asie, du nord de l'Amérique du Nord et du sud de l'Amérique du Nord et était associé à une intense dépression des Aléoutiennes de grande échelle. À notre connaissance, il s'agit de la première analyse à établir la présence de motifs régionaux de covariation de l'abondance des saumons à l'échelle de la ceinture du Pacifique Nord. Cette analyse souligne l'existence de covariations à l'échelle de ce bassin de l'abondance des saumons sauvages, covariations qui sont associées à des motifs climatiques spatialement cohérents qui varient selon la région, dans le Pacifique Nord. [Traduit par la Rédaction]

Introduction

Climate can have large impacts on the abundance and distribution of marine species. Marine species may be directly affected by environmental changes through variability in growth, reproduction, survival, and distribution and indirectly affected through changes in top-down and bottom-up trophic interactions (Roessig et al. 2004; Perry et al. 2005; Drinkwater et al. 2010). Retrospective analyses of biological and physical data from across the North Pacific have contributed to the identification of both large- and local-scale environmental processes important to trends and variations in the productivity of marine ecosystems of the North Pacific (e.g., Hare and Francis 1995; Hare and Mantua 2000; Litzow and Mueter 2009).

The abundance and productivity of Northeast Pacific salmon (*Oncorhynchus* spp.) has been related to both large- and local-scale environmental indices (e.g., Hare and Francis 1995; Hare and Mantua 2000; Mueter et al. 2002). Environmental conditions during the early marine stages may be especially important because early marine growth of juvenile salmon during their first summer

at sea influences survival during late fall and winter, so prey availability and quality during this critical period is related to subsequent adult salmon abundance (Moss et al. 2005; Farley et al. 2007; Cross et al. 2008). Other factors during the early ocean period, such as predation mortality, may also be important contributors to subsequent adult salmon abundance (Parker 1962). Marine food-web conditions during this period may be shaped by the physical environment over several years and correlated with large-scale environmental indices.

Patterns in North Pacific salmon production have been particularly well studied because Pacific salmon support major commercial, subsistence, and recreational fisheries around the North Pacific Rim, and historical catch and escapement estimates are available for many population groups over multiple decades and across broad geographic regions. Analysis of catches of pink salmon (*Oncorhynchus gorbuscha*), chum salmon (*Oncorhynchus keta*), and sockeye salmon (*Oncorhynchus nerka*) in the United States, Canada, Japan, and Russia for 1925–1989 indicated a common production pattern among species throughout the North Pacific (Beamish and Bouillon 1993). Multidecadal variations in this basin-scale

M.M. Stachura and N.J. Mantua.* School of Aquatic and Fishery Sciences, University of Washington, Box 355020, Seattle, WA 98195, USA.
M.D. Scheuerell. Fish Ecology Division, Northwest Fisheries Science Center, National Marine Fisheries Service, National Oceanic and Atmospheric Administration, Seattle, WA 98112, USA.

Corresponding author: Megan M. Stachura (e-mail: mstachur@u.washington.edu).
*Present address: Southwest Fisheries Science Center, National Marine Fisheries Service, National Oceanic and Atmospheric Administration, 110 Shaffer Road, Santa Cruz, CA 95060, USA.

Fig. 1. Approximate geographic locations of the regional stocks groups. Modified from Ruggerone et al. (2010); reprinted by permission of Taylor & Francis.
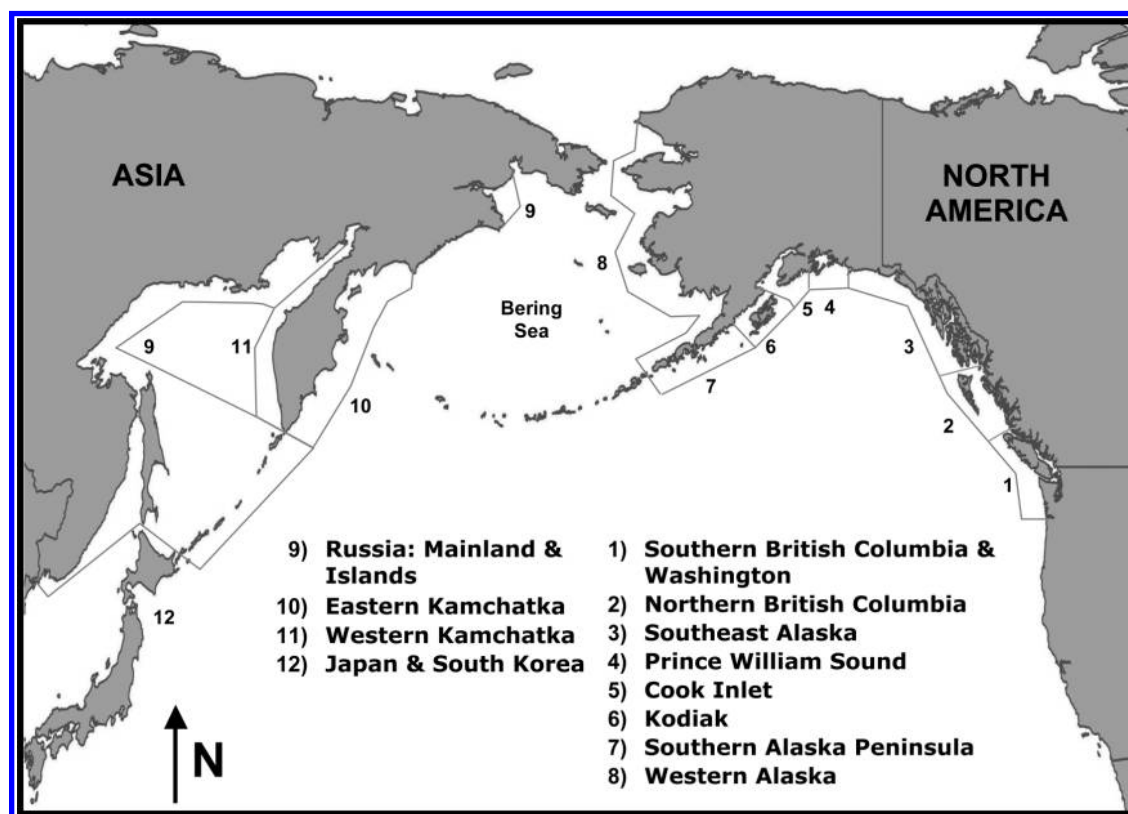
pattern of salmon production was related to variations in the intensity of the Aleutian Low atmospheric pressure system (Beamish and Bouillon 1993). Large-scale covariation between Alaska and US west coast Pacific salmon production has also been related to physical forcing through the Pacific Decadal Oscillation (PDO), the dominant pattern of North Pacific sea surface temperature (SST) variability that is also linked with variations in the Aleutian Low (Mantua et al. 1997; Hare et al. 1999).

Regional differences in relationships between salmon production and environmental variability have also been identified. Several studies have shown positive covariation in productivity among Northeast Pacific pink, chum, and sockeye salmon stocks across scales of several hundred kilometres, but not on larger scales (Peterman et al. 1998; Pyper et al. 2001, 2002; Mueter et al. 2007). Moreover, positive coastal SST anomalies were associated with increased productivity of pink, chum, and sockeye salmon in Alaska and decreased productivity for stocks of these species in Washington and British Columbia (Mueter et al. 2002).

Ruggerone et al. (2010) assembled 54-year time series (1952–2005) of catch and spawner abundance estimates for 34 regional groups of pink, chum, and sockeye salmon from across the North Pacific. They used these estimates to evaluate trends in abundance and density-dependent interactions between wild and hatchery salmon at sea, but did not examine patterns of covariation among the different population groups and species of salmon. Further analysis of these data can aid in understanding regional and large-scale patterns of salmon abundance within the North Pacific.

We apply ordination techniques to the 34 time series of regional salmon abundance from Ruggerone et al. (2010) to identify patterns of salmon production and associated environmental patterns of the North Pacific. Ordination techniques allow the variance in a large number of variables to be represented in a smaller number of dimensions with a minimal loss of information. We hypothesize that a small number of common patterns account for

a large proportion of the total variance of North Pacific salmon abundance and that these patterns are associated with basin-scale patterns of climate variation. We test this hypothesis using the regional pink, chum, and sockeye salmon abundance data compiled by Ruggerone et al. (2010), environmental indices, and gridded historical observations of SST and atmospheric sea level pressure (SLP). Pink, chum, and sockeye salmon accounted for more than 93% of the total salmon abundance returning from the ocean, so they represent most of the salmon within North Pacific ecosystems (Ruggerone et al. 2010). We expect that the common patterns in abundance will be related to environmental variability during the marine stages, especially the early marine stages, because of large-scale environmental influences similarly impacting habitats shared by regional population groups.

Materials and methods

Data

We obtained abundance estimates of wild Pacific salmon, calculated as the sum of catch plus spawning abundance data, from 1952 to 2005 assembled by Ruggerone et al. (2010). These data included pink, chum, and sockeye salmon from 12 regions spanning eastern Asia and western North America (N. Am.; Fig. 1). Across these species and regions, data were available for a total of 34 regional population groups (the Japan and South Korea region did not have data for chum and sockeye salmon). These abundance estimates should provide a better index of salmon recruitment than catch data alone because they are less influenced by such factors as changes in fishing effort and harvest policies, although salmon catch and abundance patterns have shown high correlation (Eggers and Irvine 2007). The year of ocean entry is widely recognized as a period of high mortality during which year-class strength is primarily determined (Peterman 1987; Beamish and Mahnken 2001). Thus, we aligned salmon abundance time series

Table 1. Description of environmental time series used in analyses.

Abbreviation	Name	Description	Data source	Reference
AO	Arctic Oscillation Index	Dominant pattern of sea level pressure variability north of 20°N in winter (January–March)	NOAA Climate Prediction Center	Thomson and Gower 1998
MEIW	Multivariate El Niño–Southern Oscillation Winter Index	Dominant pattern of variability of six observed variables over the tropical Pacific in winter (October–March)	NOAA Earth System Research Laboratory	Wolter and Timlin 1998
MEIS	Multivariate El Niño–Southern Oscillation Summer Index	Dominant pattern of variability of six observed variables over the tropical Pacific in summer (April–September)	NOAA Earth System Research Laboratory	Wolter and Timlin 1998
NPGOW	North Pacific Gyre Oscillation Winter Index	Second dominant pattern of sea surface height variability in the Northeast Pacific in winter (October–March)	Emanuele Di Lorenzo, Georgia Institute of Technology	Di Lorenzo et al. 2008
NPGOS	North Pacific Gyre Oscillation Summer Index	Second dominant pattern of sea surface height variability in the Northeast Pacific in summer (April–September)	Emanuele Di Lorenzo, Georgia Institute of Technology	Di Lorenzo et al. 2008
PDOW	Pacific Decadal Oscillation Winter Index	Dominant pattern of North Pacific sea surface temperature variability north of 20°N in winter (October–March)	University of Washington, Joint Institute for the Study of the Atmosphere and Ocean	Mantua et al. 1997
PDOS	Pacific Decadal Oscillation Summer Index	Dominant pattern of North Pacific sea surface temperature variability north of 20°N in summer (April–September)	University of Washington, Joint Institute for the Study of the Atmosphere and Ocean	Mantua et al. 1997
EPNP	East Pacific–North Pacific Index	Teleconnection index with positive phase associated with a southward shift and intensification of the Pacific jet stream measured in summer (April–September)	NOAA Climate Prediction Center	Barnston and Livezey 1987
ALPI	Aleutian Low Pressure Index	Index of the relative intensity of the Aleutian Low pressure system in winter (December–March)	Fisheries and Oceans Canada	Beamish et al. 1997
NPHPI	North Pacific High Pressure Index	Index of NCEP Reanalysis sea level pressure at 30–42.5°N, 135–180°W in summer (April–September)	NOAA Earth System Research Laboratory	Kalnay et al. 1996

Note: Indices spanning 2 years are assigned to the year corresponding to January.

based on each species' general life history patterns by lagging the time series by the difference between the mean age of spawning and the mean age of ocean entry as a smolt (i.e., 1, 2, and 3 years for pink, sockeye, and chum, respectively) (Groot and Margolis 1991). After aligning all time series for all species, we ultimately used ocean entry years 1951–2002 in this analysis.

We standardized the log-transformed abundance time series for each of the 34 regional population groups to have a mean of 0 and a standard deviation of 1. Pink salmon have a strict 2-year life cycle, which creates genetically distinct populations in even and odd years, and large differences exist among run sizes in even and odd years for some regions. To reduce the signal of this 2-year cycle in the time series for each population group, pink salmon even and odd year abundance values were standardized independently, then recombined into a single continuous annual time series within each population group region. We considered the even and odd year pink salmon regional groups as a single time series with the assumption that shared regional environmental processes impact their abundance.

We compiled 10 environmental indices for the North Pacific to analyze how they relate to patterns of salmon abundance (Table 1). We also used gridded SST and SLP data across the North Pacific to investigate the spatial relationship of the patterns in salmon abundance with environmental variability. Monthly values of NOAA Extended Reconstructed SST at a 2° × 2° spatial resolution and NCEP Reanalysis SLP at a 2.5° × 2.5° spatial resolution were provided by the NOAA–OAR–ESRL PSD, Boulder, Colorado, USA, from their web site at http://www.esrl.noaa.gov/psd/ (Kalnay et al. 1996; Smith et al. 2008). We calculated extended winter (October–March, for year corresponding to January) and summer (April–September) averages of these data for the North Pacific Ocean for

mapping to allow for investigation of environmental drivers of salmon abundance patterns.

Ordination methods

Several ordination methods have been previously employed to identify shared patterns in marine productivity across populations. Principal component analysis (PCA) is an ordination technique that reduces the number of variables in a data set into a fewer number of dimensions that are linear combinations of the original variables. PCA has been previously used in identification of the patterns in Northeast Pacific salmon catch data (Hare et al. 1999; Litzow and Mueter 2009). Nonmetric multidimensional scaling (NMDS) is an ordination technique that attempts to arrange objects in a low-dimensional space such that the distances in the ordination space are close to the ranked distances of the original data set. This method has been shown to be more robust to the nonlinearities inherent in ecological data sets than linear ordination techniques such as PCA (Minchin 1987). NMDS has been used previously in identification of changes in species composition of demersal fish and shrimp communities in the Gulf of Alaska (Mueter and Norcross 2000). Dynamic factor analysis (DFA) is a dimension-reduction technique designed specifically for time series data that models multiple time series in terms of their common trends and additional explanatory variables (Zuur et al. 2003a). DFA has been used in several applications to estimate common trends in fisheries time series (Zuur et al. 2003b; Zuur and Pierce 2004; Devine and Haedrich 2011). We used these three techniques to identify temporal patterns in North Pacific salmon abundance and evaluate their relationship with the marine environment. We calculated the Mantel statistic to compare the Euclidean distance between objects in ordination space among the

three ordination methods and used a Mantel test to determine whether consistent patterns were identified among methods.

PCA

PCA concentrates most of the variance in a large data set into a smaller number of easily interpreted patterns that are a linear combination of the original data set. The principal components (PCs, also called scores) give the temporal variability in the data set. The eigenvectors (also called loadings) describe the weights by which the individual salmon abundance time series are multiplied in the calculation of the PCs. Positive loadings indicate the time series has a positive correlation with the PC and negative loadings indicate a negative correlation. The eigenvalues indicate the amount of variance explained by each PC.

The first few PCs explained most of the variance of the data set and were used to describe the major patterns of variability. The statistical significance of the first 10 PCs was used to determine the appropriate number of PCs to examine based on two commonly used methods, the broken stick model and a Monte Carlo permutation test of significance with 1000 permutations (Legendre and Legendre 1998). Overlap in the sampling error of the eigenvalues indicates the patterns described by the PCs are potentially mixed and noninterpretable. We calculated the sampling errors of the PCs using the formula of North et al. (1982) to ensure nonoverlap of the PCs examined. PCA was implemented in the R "stats" package (R Development Core Team 2012).

To identify environmental variables related to the patterns in salmon abundance, we calculated Pearson correlation coefficients and the corresponding statistical significance between the PC axes and environmental variables. We corrected for autocorrelation in the test of statistical significance using the procedure recommended by Pyper and Peterman (1998). We also used the Bonferroni correction to correct for the large number of correlations investigated. For all statistical tests, the level of significance was 0.05.

NMDS

NMDS attempts to arrange objects in a low-dimensional space such that the distances in the ordination space are close to the ranked distances of the original data set. The configuration of the points within the ordination space is iteratively adjusted to improve the correspondence with the ranked distances of the original data set until no improvement in the fit is observed. The NMDS axes (also called scores) give the temporal variability in the data set. The loadings indicate the correlation of the individual salmon regional abundance time series with the NMDS axes. We used Euclidean distance, which follows the equation

$$(1) \qquad D(\boldsymbol{y}_1, \boldsymbol{y}_2) = \sqrt{\sum_{t=1}^{p} (y_{1,t} - y_{2,t})^2}$$

where the distance between salmon abundance time series $\boldsymbol{y}_1$ and $\boldsymbol{y}_2$ ($D(\boldsymbol{y}_1, \boldsymbol{y}_2)$) is a function of the squared difference between the time series at time t summed over the p years of data (Legendre and Legendre 1998).

In NMDS the number of dimensions, or axes, of the ordination must be specified. The stress, a goodness-of-fit criterion that measures the discrepancy between the distance in ordination space and the distances of the original data set, was used to determine the appropriate number of dimensions for the ordination. The stress decreases with an increase in the number of dimensions, and a value of 20% or less is considered interpretable (Clarke 1993). NMDS was implemented in the R (R Development Core Team 2012) "vegan" package (Oksanen et al. 2011).

We also calculated Pearson correlation coefficients and their corresponding statistical significance accounting for autocorrelation and the Bonferroni correction between the NMDS axes and environmental variables.

DFA

We used DFA to model the shared trends in abundance among the stocks as a linear combination of common trends and the effect of environmental drivers. DFA allows the common patterns among N time series to be characterized with many fewer M trends. Following Zuur et al. (2003b), the DFA model can be written as

$$(2) \qquad \boldsymbol{y}_t = \mathbf{Z}\boldsymbol{\alpha}_t + \mathbf{D}\boldsymbol{x}_t + \boldsymbol{e}_t$$

$$(3) \qquad \boldsymbol{\alpha}_t = \boldsymbol{\alpha}_{t-1} + \boldsymbol{f}_t$$

The $N \times 1$ vector of data observed at time t ($\boldsymbol{y}_t$) are modeled as a linear combination of the $M \times 1$ vector of latent trends ($\boldsymbol{\alpha}_t$), $P \times 1$ vector of explanatory variables ($\boldsymbol{x}_t$), and observation (sampling) errors ($\boldsymbol{e}_t$). Both $\boldsymbol{e}_t$ and $\boldsymbol{f}_t$, the vector of process errors at time t, followed multivariate normal distributions with mean vectors 0 and variance–covariance matrices $\mathbf{R}$ and $\mathbf{Q}$, respectively. The matrices $\mathbf{Z}$ and $\mathbf{D}$ contain the stock-specific loadings on the trends and explanatory effects, respectively. These loadings can be compared to determine which common trends and environmental variables explain the abundance variability for a particular region and which regions have shared abundance variability.

Although DFA and PCA are similar, there are some important distinctions. In PCA the trends must be straight lines that are orthogonal to each other, whereas in DFA the trends are smooth random walks that can take many shapes. DFA also allows for a variety of forms of the covariance between time series ($\mathbf{R}$) to account for interactions between stock groups.

Three forms of the observation error variance–covariance matrix $\mathbf{R}$ were tested: a diagonal matrix with equal variance and zero covariance, a diagonal matrix with unequal variance and zero covariance, and a nondiagonal matrix with equal variance and equal covariance. Using a diagonal matrix $\mathbf{R}$ can lead to common trends that are only related to a few response variables (Zuur et al. 2003b). For that reason, the variance–covariance matrix that included nonzero covariance was also considered, in which the off-diagonal elements of the variance–covariance matrix represent joint information in the regional salmon abundance time series that cannot be explained with other terms (Zuur et al. 2003b).
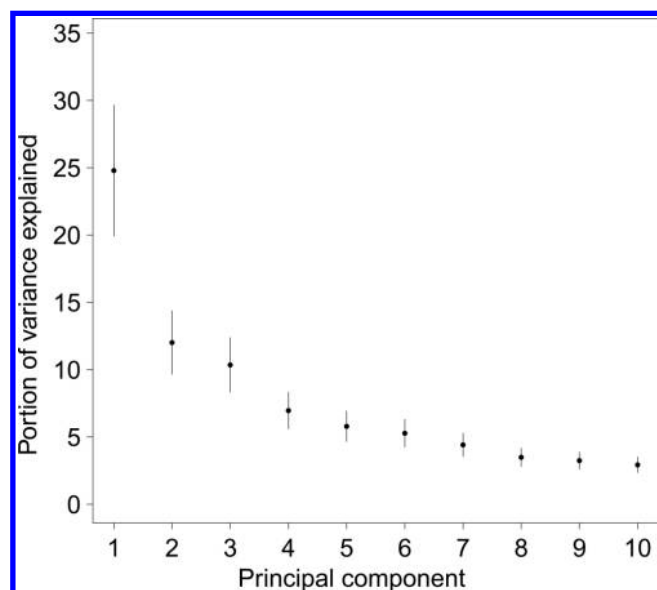
Models including the 10 environmental indices individually as explanatory variables ($\boldsymbol{x}_t$) were also tested. Three forms of the stock-specific loadings ($\mathbf{D}$) on the explanatory variables were tested. The first consisted of independent loadings estimated for each population group, the second consisted of three loadings estimated that were equal for all population groups of each species, and the third consisted of a single loading estimated that was equal for all population groups across all species. The form of $\mathbf{R}$ in the best model chosen from those without explanatory variables was the same form used in the models with explanatory variables.

One to six common trends (M) were investigated for each of the model forms (with and without covariates). The small-sample Akaike information criterion (AIC$_c$) was used as a measure of goodness of fit to compare the models (Hurvich and Tsai 1989). Other model diagnostics, including examination of the residuals, model fits, trends, and factor loadings, were also used in model evaluation and selection. Minimizing the number of trends used in analysis was also important to ease interpretation. DFA was implemented in the R (R Development Core Team 2012) "MARSS" package (Holmes et al. 2013).

Physical variable mapping

Compositing, or superposed epoch analysis, is a method commonly used in climate science to identify environmental conditions associated with events, such as explosive volcanic eruptions or an El

230

Can. J. Fish. Aquat. Sci. Vol. 71, 2014

Fig. 2. Plot of the portion of total variance in the salmon abundance data explained by the first 10 principal components from principal component analysis. The sampling error bars were computed using the formula of North et al. (1982).

Fig. 3. Scores of the (*a*) first, (*b*) second, and (*c*) third principal components (solid), nonmetric multidimensional scaling axes (dashed), and dynamic factor analysis trends (dotted).

Niño – Southern Oscillation event onset (Portman and Gutzler 1996). In compositing, the data are separated into categories or time periods (epochs) and the mean conditions for the different categories are compared. This method makes no assumptions of linearity and is good at separating small signals from noise. For compositing, the years corresponding to the highest one-third and lowest one-third of the PCs, NMDS axes, and DFA trends were identified. Mean extended winter (October–March, for year corresponding to January) and summer (April–September) SST and SLP maps for these years were plotted as composite anomalies from the mean values over the time period of analysis (1951–2002). We visually inspected these maps to identify patterns in the physical environment related to the patterns of salmon abundance.

Results

We found three primary patterns of temporal variation in salmon abundance across the North Pacific that accounted for a large proportion of the total variability in the data. The first three PCs accounted for 25%, 12%, and 10% of the total variance of the data, respectively, together accounting for 47% of the total variance (Fig. 2). These PCs were significant based on both the broken stick model and Monte Carlo permutation tests. The sampling error of the first PC does not overlap with any other PCs. While the sampling error of the second and third PCs overlap, the sampling error of the third PC only marginally overlaps with that of the fourth PC, so the patterns should not be mixed with higher order PCs (Fig. 2) (North et al. 1982).

A three-dimensional NMDS resulted in a stress of 13% and was chosen to optimize clarity of interpretation while maintaining reliably interpretable results of the NMDS analysis and to be consistent with the number of PCs analyzed. The linear fit of the distances in ordination space to the distances of the original data set had an R^2 value of 0.88, also indicating the ordination provides a reliable interpretation of the original data set.

We found overwhelming support from the data for a DFA model with four common trends among the 34 population groups with unequal variance and no covariance among stock groups. None of
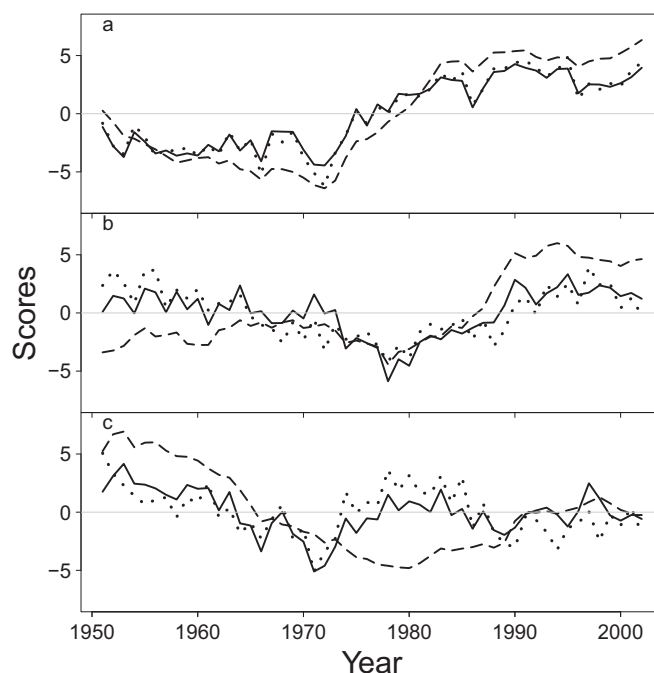
the models that included explanatory variables, with independent loadings for each population group, equal loadings for all population groups of each species, and equal loadings for all population groups across all species, were better based on AIC_c model selection than the best model without explanatory variables. The PC and NMDS axes investigated also did not have a significant correlation with any of the environmental indices (Table S1[1]). For ease of interpretation, only three of the four trends from the best DFA model that were most consistent with the PCs and NMDS axes are presented.

The Mantel statistic between the axes scores distances from PCA and NMDS was very high ($r = 0.92$, $p < 0.001$). The Mantel statistic for PCA and DFA ($r = 0.84$, $p < 0.001$) and DFA and NMDS ($r = 0.79$, $p < 0.001$) were lower but still highly significant. Limited NMDS and DFA results are presented, but they are consistent with the PCA results except where noted.

The first dominant pattern consisted of the first PC (PC1), first NMDS axis, and first DFA trend. Across the three methods, this pattern exhibited a shift from low to high scores starting in the early, mid, or late 1970s (Fig. 3). Most of the N. Am. population groups had positive loadings on the first pattern, with several groups exhibiting moderately strong loadings (Fig. 4, Fig. S1[1]). Cook Inlet pink and chum salmon were the only N. Am. groups that had negative loadings on this PC. Several eastern and western Kamchatka groups also had positive loadings on the first DFA trend, which was not observed in the PCA or NMDS results (Fig. S2[1]). Composite maps of SST and SLP anomalies for years of low values of the first pattern were associated with cooler SSTs in the coastal waters of Russia and the Bering Sea and higher winter SLPs over the Aleutian Islands (Fig. 5, Fig. S3, Fig. S4[1]). High values of the first pattern were associated with warmer coastal temperatures through much of the North Pacific and lower winter SLP over the Aleutian Islands. SST anomalies were especially strong in the far eastern Bering Sea in winter, for composites of both the highest and lowest values of this pattern (positive and negative

---

Fig. 4. Loadings on the first principal component. The size of the circle is proportional to the magnitude of the loading, the different shading indicates the sign of the loading, the letter indicates the species (P, pink; C, chum; and S, sockeye), and the location corresponds to the region of the salmon population group.
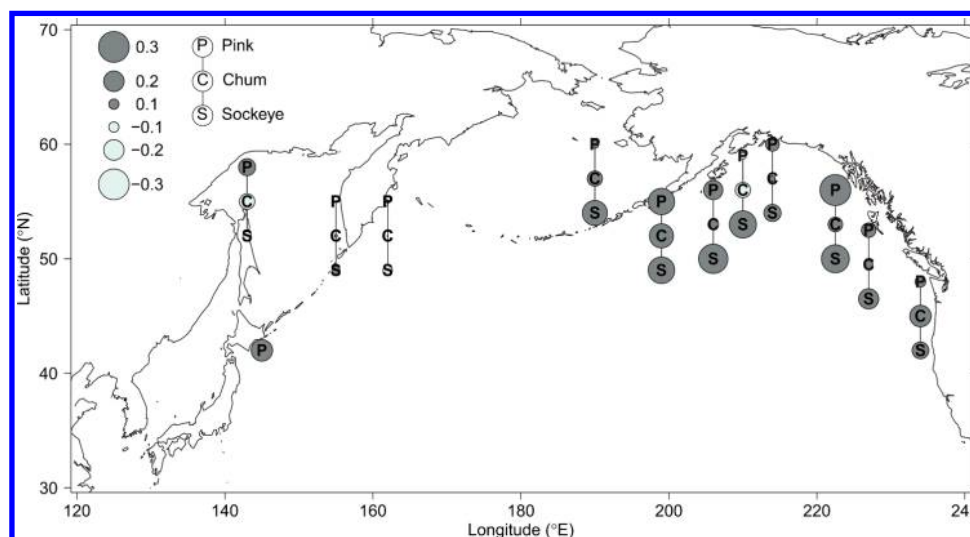

Fig. 5. Composite maps of the mean sea surface temperature (SST; °C) and sea level pressure (hPa); shown as contour lines with dashed lines indicating negative anomalies and solid lines indicating zero or positive anomalies) anomalies from the longterm mean (1951–2002) for (*a*) winter (October–March, for year corresponding to January) for years corresponding to the lowest one-third of principal component one (PC1) scores, (*b*) summer (April–September) for years corresponding to the lowest one-third of PC1 scores, (*c*) winter for years corresponding to the highest one-third of PC1 scores, and (*d*) summer for years corresponding to the highest one-third of PC1 scores.
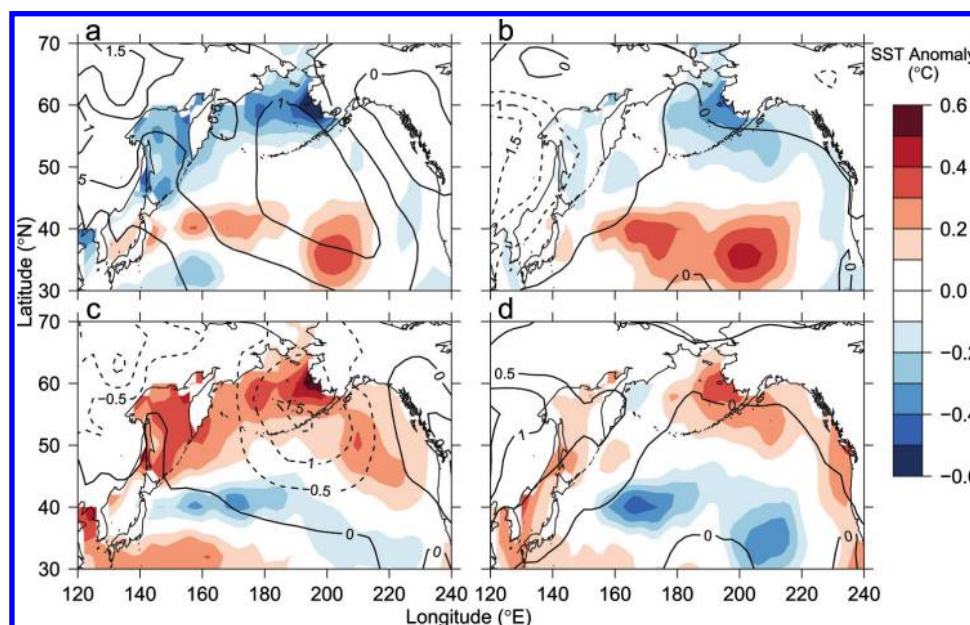
anomalies, respectively), and this subregional expression was also evident in summer but with weaker SST anomalies.

The second dominant pattern consisted of the second PC (PC2), second NMDS axis, and second DFA trend. PC2 had low scores from the mid-1970s to the late 1980s, with moderate and high scores in the remaining periods (Fig. 3). The second NMDS axis had a longer period of low scores from the mid-1960s to the late 1980s. The second DFA trend had low values through the early 1980s, when there was a shift to high trend values. Most Asian population groups had positive loadings on this pattern, while N. Am. population groups tended to have negative loadings, except the Southeast Alaska, British Columbia, and Washington groups (Fig. 6, Fig. S5[1]). This pattern was less clear in the DFA loadings because a few Asian populations (western Kamchatka pink and

chum salmon and eastern Kamchatka chum salmon) had negative loadings (Fig. S6[1]). Low values of the second pattern were associated with cooler temperatures around Japan and the central North Pacific, warmer temperatures in the eastern Bering Sea and central Gulf of Alaska, and negative winter SLP anomalies over the North Pacific (Fig. 7, Fig. S7[1]). Low values of the second DFA trend were instead associated with cooler winter temperatures in the Bering Sea and the coastal waters around Russia and warmer winter temperatures around Japan (Fig. S8[1]). High values of the second pattern were associated with warmer temperatures throughout much of the North Pacific, especially in the eastern Bering Sea and waters around Russia for the second DFA trend.

The third dominant pattern consisted of the third PC (PC3), third NMDS axis, and third DFA trend. This PC had high scores through the

Fig. 6. Loadings on the second principal component. The size of the circle is proportional to the magnitude of the loading, the different shading indicates the sign of the loading, the letter indicates the species (P, pink; C, chum; and S, sockeye), and the location corresponds to the region of the salmon population group.
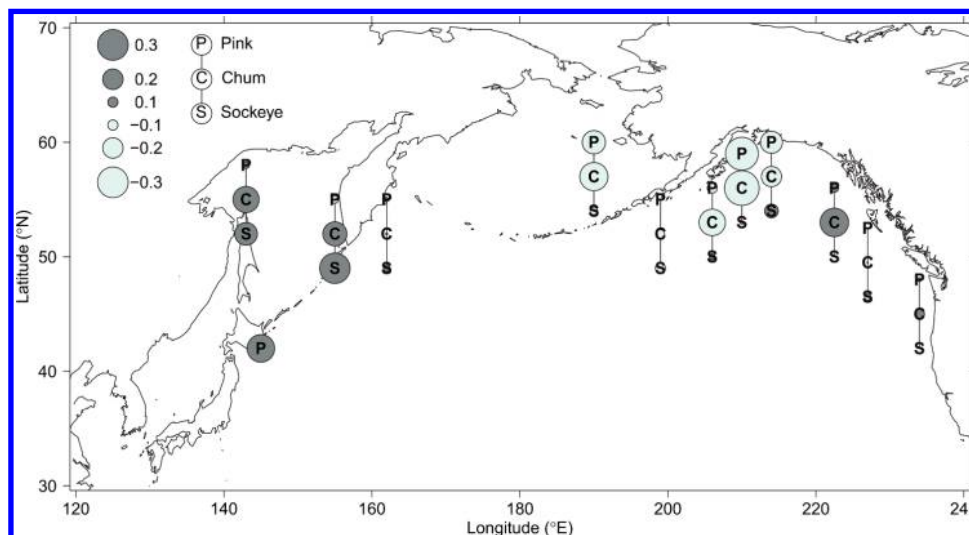

Fig. 7. Composite maps of the mean sea surface temperature (SST; °C) and sea level pressure (hPa); shown as contour lines with dashed lines indicating negative anomalies and solid lines indicating zero or positive anomalies) anomalies from the longterm mean (1951–2002) for (*a*) winter (October–March, for year corresponding to January) for years corresponding to the lowest one-third of principal component two (PC2) scores, (*b*) summer (April–September) for years corresponding to the lowest one-third of PC2 scores, (*c*) winter for years corresponding to the highest one-third of PC2 scores, and (*d*) summer for years corresponding to the highest one-third of PC2 scores.
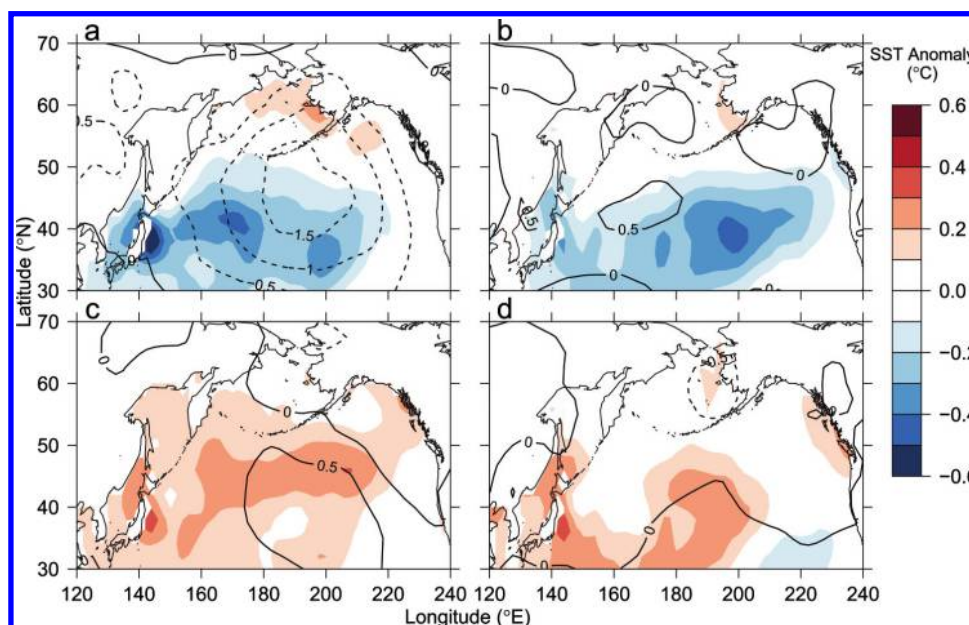
early 1960s, followed by low scores through the mid-1970s and moderate scores in the remaining time period (Fig. 3). The third DFA trend also showed a decrease from high to low values in the 1960s, but showed an extended period of low values from the late 1960s to the late 1980s, with moderate values in the remaining period. Most Russian and western Gulf of Alaska (southern Alaska Peninsula, Kodiak, Cook Inlet, and Prince William Sound) stock groups had positive loadings on the third pattern, with pink and chum stocks having the strongest loadings (Fig. S9, Fig. S10[1]). Few N. Am. population groups had strong loadings on the third DFA trend, indicating this trend mostly captured variations in the Russian population groups (Fig. S11[1]). Low values of PC3 were associated with cooler coastal SSTs in the Northeast Pacific, especially in the Gulf of Alaska in summer, while high values were associated with warmer SSTs in the Gulf of

Alaska and along British Columbia, Washington, and Japan, cooler winter SSTs in the Bering Sea and along Russia, and negative winter SLP anomalies in the Northeast Pacific (Fig. S12[1]). The third NMDS axis was associated with weaker SST and SLP anomalies, and the third DFA trend was associated with weaker SST and SLP anomalies in the Northeast Pacific but stronger anomalies around Russia and Japan (Fig. S13, Fig. S14[1]).

Discussion

We used three different multivariate analysis methods to identify common patterns in North Pacific pink, chum, and sockeye salmon abundance. Our analyses identified a leading pattern exhibited by many of the population groups in N. Am. and a second

pattern that captures differences among (*i*) Asian, (*ii*) western and central Alaska, and (*iii*) Southeast Alaska, British Columbia, and Washington population groups.

The dominant patterns and trends in salmon abundance were robust to the three different analysis methods used in this study. While the results of the PCA and NMDS were very similar, the DFA results differed in a few important ways. DFA, which is especially designed for use with time series data, identified trends that had greater autocorrelation than the patterns identified by PCA and NMDS. This is due to the lag-one autocorrelation that is part of the modeling of the trends in DFA (eq. 2). The second DFA trend also showed a weaker difference between the Asian and western and central Alaska population groups than the PCA and NMDS results with negative loadings on some Asian population groups, indicating further analysis of the second pattern may be warranted. The DFA models tested also included environmental indices as explanatory variables, but a model without any covariates was chosen as the best model. The poor fits of the models with these environmental covariates may be due to the high correlation of the abundance time series with these covariates for only a small portion of the population groups. Further testing of DFA models that include these explanatory variables for only a subset of the population groups or with equal loadings for a subset of the population group that are most similarly impacted may provide better model fits. In this analysis we did not investigate regional environmental variables, as opposed to large-scale basin-wide environmental variables, but previous research has shown regional factors influence shared patterns of covariation among stocks (e.g., Peterman et al. 1998; Pyper et al. 2001). Additional DFA modeling that includes both regional and large-scale environmental variables may improve model fits.

The leading pattern in the salmon abundance data captures variability in many N. Am. population groups, especially those from Alaska. The composite SST anomaly patterns for years of the highest and lowest values of PC1 feature anomalies across both the eastern and western North Pacific, particularly in winter, and especially strong anomalies are concentrated in the eastern Bering Sea and northern Gulf of Alaska. Although previous analyses have associated the dominant pattern of N. Am. salmon abundance with the PDO, this SST pattern is much more concentrated than that associated with the PDO, which has much of its signature across the broader subarctic North Pacific. The dominant pattern of abundance may also be related to a regional expression of large-scale environmental patterns.

The change in SST associated with the leading pattern of salmon abundance is closely related to low-frequency, oscillatory temperature changes in the SST of the North Pacific, captured in part by the PDO. The Gulf of Alaska and eastern Bering Sea winter SST conditions associated with this dominant pattern of salmon abundance had cooler conditions than the long-term (1900–2012) mean in several recent years (2008, 2009, and 2012) (Fig. 8). If environmental conditions related to SST in this region are causing changes in this salmon production pattern, the recent cool period may be a harbinger of declining salmon abundance for many pink, chum, and sockeye salmon stocks in Alaska and northern British Columbia.

The first pattern of salmon abundance also showed a positive shift in the mid-1970s, which corresponds to a widely recognized regime shift across several Northeast Pacific ecosystems (Hare and Mantua 2000). Previous studies have shown that the increase in productivity and abundance of the N. Am. salmon stocks in the late 1970s coincided with an increase in productivity of plankton and many marine fish species, supporting the idea of an increase in pelagic marine production during this time period (Francis et al. 1998; Anderson and Piatt 1999). Moreover, a study of the food habits of sockeye, chum, and pink salmon conducted in 2002–2006 found that salmon feeding conditions, growth, and survival in the eastern Bering Sea were more favorable in relatively warm years, as compared with cool years (Davis et al. 2009).

Fig. 8. Plot of the mean winter (October–March, for year corresponding to January) sea surface temperature in the Gulf of Alaska and eastern Bering Sea (50–60°N, 180–220°E) and principal component one from principal component analysis of the salmon abundance data.
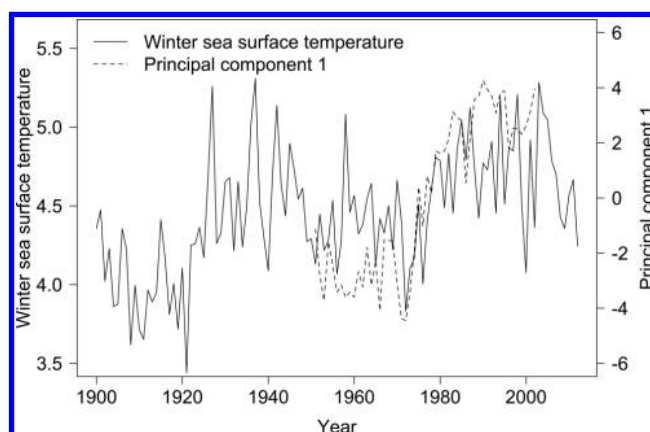

The more pronounced winter SST and SLP anomalies associated with the first pattern may point to the importance of freshwater conditions. Warm periods in Alaska's marine waters correlate with warm periods in Alaska's freshwater habitat that appear to be favorable for many pink, chum, and sockeye salmon populations (Schindler et al. 2005). For example, the extended warm period from the late 1970s to early 2000s featured earlier spring ice-breakup and warmer summer water temperatures in a southwestern Alaskan lake; conditions that relate to greater summer zooplankton abundance and juvenile sockeye salmon growth (Schindler et al. 2005).

While Beamish and Bouillon (1993) focused on one common pattern in catch of salmon across the United States, Canada, Japan, and Russia, our analysis indicates a secondary pattern of variability exists as distinct patterns among the northern and southern N. Am. regions and Asia. Based on the observed general geographical patterns in loadings, we created three larger aggregate groups of total abundance for purposes of comparison: (*i*) southern N. Am. (1–3 in Fig. 1), (*ii*) northern N. Am. (4–8 in Fig. 1), and (*iii*) Asia (9–12 in Fig. 1). These aggregate abundances, which were standardized to a mean of 0 and standard deviation of 1 for comparison, showed the greatest difference between the Asian and both N. Am. regions, with the Asian groups having higher abundance in the 1950s and lower abundance in the mid-1970s to 1980s (Fig. 9). There are also differences between the two N. Am. regions, with the northern group having greater abundance in the mid-1970s to mid-1980s. The opposite patterns of the Asian and northern N. Am. population groups may be due to large-scale climatic influences that simultaneously affect the North Pacific but have opposite effects on local-scale marine conditions in the Northwest and Northeast Pacific, respectively. For example, the warm phase of the PDO corresponds to warming in the Northeast Pacific but cooling in the Northwest Pacific (Mantua et al. 1997). This indicates varying and possibly opposite responses to large-scale environmental forcing by salmon stocks on the two sides of the North Pacific. There was also a varied response, although not as extreme, between the northern and southern N. Am. stocks. This difference is consistent with previous findings of opposite patterns in salmon catch (Hare et al. 1999), abundance (Peterman and Wong 1984), and productivity (Peterman et al. 1998) between these two areas.

The opposite responses by the N. Am. and Asian population groups captured by the second pattern may also indicate a role for density-dependent interactions between eastern and western populations that arises during later life stages when N. Am. and Asian

Fig. 9. The total standardized abundance of salmon for three regional groups: (*i*) southern North America, (*ii*) northern North America, and (*iii*) Asia.
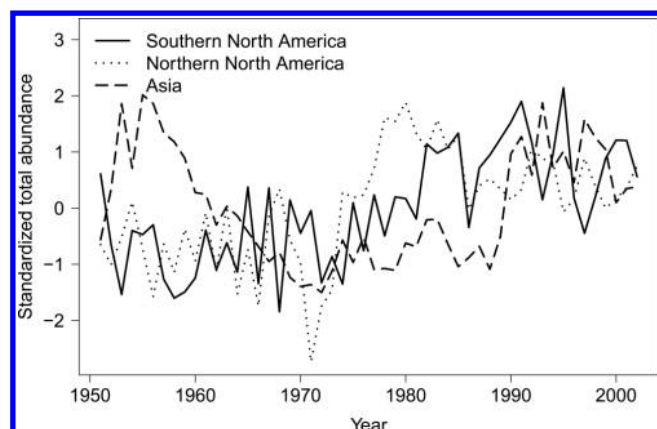
salmon have overlapping distributions in the subarctic North Pacific and Bering Sea (Ruggerone et al. 2003; Myers et al. 2007). For example, chum salmon in the central subarctic Pacific and Bering Sea were found to switch to lower quality prey in years of high Asian pink salmon abundance (Tadokoro et al. 1996). However, the stocks that Ruggerone et al. (2003) identified to have especially strong competition were eastern Kamchatka pink salmon and Bristol Bay sockeye salmon (within the western Alaska group in this analysis), which have weak loadings on the second pattern. Other Asian and N. Am. stocks do overlap in their distributions and competition among adults may be important to their growth and survival.

The third pattern of salmon abundance captures covariation in several Russian and western Gulf of Alaska population groups. High abundance for these population groups was related to warmer than average summer temperatures in the Gulf of Alaska but cooler than average winter temperatures in the Bering Sea and Sea of Okhotsk. The SLP anomalies associated with the third pattern were concentrated in the Northeast Pacific, which may have a strong influence on the environment experienced by the western Gulf of Alaska stocks that had high loadings on this pattern.

Warmer coastal temperatures have been linked to greater survival of Japanese chum salmon (Seo et al. 2011) and Alaskan pink, chum, sockeye salmon (Mueter et al. 2002; Davis et al. 2009), but decreased survival of Washington and British Columbia pink, chum, and sockeye salmon (Mueter et al. 2002). The warm temperature anomalies related to the higher abundance of the Washington and British Columbia population groups associated with the second and third patterns, although relatively weak, are not consistent with previous findings for these stocks. This may be because our analysis was based on abundance data, instead of productivity, and at a broader regional scale than the previous analysis of coastal temperature effects on these stocks (Mueter et al. 2002). Furthermore, Hare et al. (1999) identified a north–south inverse production pattern in Northeast Pacific salmon catch, but it is not surprising that we did not identify a similar pattern because our analysis did not include data for the population groups identified as the "southern" group (Washington, Oregon, and California coho (*Oncorhynchus kisutch*) and Chinook (*Oncorhynchus tshawytscha*) salmon).

Although pink, chum, and sockeye salmon have different life histories, they are similarly exposed to many environmental influences in their early marine life. We hypothesize that shared exposure in the early marine period is the mechanistic link supporting the observed covariations in abundance across these species and regions. In an analysis of the between-species correlation

in stock–recruitment residuals of pink, chum, and sockeye salmon stocks, correlations of pink and chum salmon were much stronger than sockeye salmon with either pink or chum salmon (Pyper et al. 2005; Mueter et al. 2007). In our analysis, pink and chum salmon tended to have stronger positive loadings on the third pattern than sockeye salmon, but overall there was not greater correspondence in the loadings for any subset of species. Variation in the early marine habitat used by these species may account for the varying abundance trends due to differences in local conditions, such as prey availability.

While we investigated atmospheric and oceanographic variability through the lens of salmon abundance patterns, other factors may be important for salmon abundance that were not considered here. For example, changes in harvest, hatchery practices, or freshwater habitat may contribute to abundance trends unrelated to climate and ocean variability. We did not account for influences of spawner abundance through stock–recruit relationships because of the regional scale of the data, but this is likely an important factor in the abundance of returning salmon that has been looked at in other analyses (Peterman et al. 1998; Pyper et al. 2001, 2002; Mueter et al. 2007). The biocomplexity of the salmon stocks within a region, which may be reduced because of fishing, hatcheries, and other anthropogenic influences, may also impact variability in salmon abundance (Johnson and Schindler 2012).

Our analysis of North Pacific salmon abundance identified a leading pattern similar to patterns identified in previous analyses of Northeast Pacific salmon catch and abundance, plus an additional pattern with opposite expression in northern N. Am. and Asian population groups. To our knowledge this is the first analysis that identifies regional patterns of covariation in salmon abundance around the Pacific Rim, and it highlights the existence of basin-wide covariations in wild salmon abundance that are associated with spatially coherent patterns in North Pacific climate. Identifying patterns of salmon abundance may help in understanding environmental drivers of salmon productivity, which in turn may contribute to improvements in recruitment forecasting accuracy and projections of the impacts of future climate change. The perspective gained by examination of the large-scale salmon abundance and associated climate patterns may ultimately support improved management of salmon stocks throughout the North Pacific.

Acknowledgements

References

Anderson, P.J., and Piatt, J.F. 1999. Community reorganization in the Gulf of Alaska following ocean climate regime shift. Mar. Ecol. Prog. Ser. **189**: 117–123. doi:10.3354/meps189117.

Barnston, A.G., and Livezey, R.E. 1987. Classification, seasonality and persistence of low-frequency atmospheric circulation patterns. Mon. Weather Rev. **115**(6): 1083–1126. doi:10.1175/1520-0493(1987)115<1083:CSAPOL>2.0.CO;2.

Beamish, R.J., and Bouillon, D.R. 1993. Pacific salmon production trends in relation to climate. Can. J. Fish. Aquat. Sci. **50**(5): 1002–1016. doi:10.1139/f93-116.

Beamish, R.J., and Mahnken, C. 2001. A critical size and period hypothesis to explain natural regulation of salmon abundance and the linkage to climate and climate change. Prog. Oceanogr. **49**(1–4): 423–437. doi:10.1016/S0079-6611(01)00034-9.

Beamish, R.J., Neville, C.-E.M., and Cass, A.J. 1997. Production of Fraser River sockeye salmon (*Oncorhynchus nerka*) in relation to decadal-scale changes in the climate and the ocean. Can. J. Fish. Aquat. Sci. **54**(3): 543–554. doi:10.1139/f96-310.

Clarke, K.R. 1993. Non-parametric multivariate analyses of changes in com-

munity structure. Aust. J. Ecol. **18**(1): 117–143. doi:10.1111/j.1442-9993.1993.tb00438.x.

Cross, A.D., Beauchamp, D.A., Myers, K.W., and Moss, J.H. 2008. Early marine growth of pink salmon in Prince William Sound and the coastal Gulf of Alaska during years of low and high survival. Trans. Am. Fish. Soc. **137**(3): 927–939. doi:10.1577/T07-015.1.

Davis, N.D., Volkov, A.V., Efimkin, A.Y., Kuznetsova, N.A., Armstrong, J.L., and Sakai, O. 2009. Review of BASIS salmon food habits studies. N. Pac. Anadr. Fish Comm. Bull. **5**: 197–208.

Devine, J.A., and Haedrich, R.L. 2011. The role of environmental conditions and exploitation in determining dynamics of redfish (*Sebastes* species) in the Northwest Atlantic. Fish. Oceanogr. **20**(1): 66–81. doi:10.1111/j.1365-2419.2010.00566.x.

Di Lorenzo, E., Schneider, N., Cobb, K.M., Franks, P.J.S., Chhak, K., Miller, A.J., McWilliams, J.C., Bograd, S.J., Arango, H., Curchitser, E., Powell, T.M., and Rivière, P. 2008. North Pacific Gyre Oscillation links ocean climate and ecosystem change. Geophys. Res. Lett. **35**(8): L08607. doi:10.1029/2007GL032838.

Drinkwater, K.F., Beaugrand, G., Kaeriyama, M., Kim, S., Ottersen, G., Perry, R.I., Pörtner, H.O., Polovina, J.J., and Takasuka, A. 2010. On the processes linking climate to ecosystem changes. J. Mar. Syst. **79**(3–4): 374–388. doi:10.1016/j.jmarsys.2008.12.014.

Eggers, D.M., and Irvine, J.R. 2007. Trends in abundance and biological characteristics for north Pacific sockeye. N. Pac. Anadr. Fish Comm. Bull. **4**: 53–75.

Farley, E.V., Moss, J.H., and Beamish, R.J. 2007. A review of the critical size, critical period hypothesis for juvenile Pacific salmon. N. Pac. Anadr. Fish Comm. Bull. **4**: 311–317.

Francis, R.C., Hare, S.R., Hollowed, A.B., and Wooster, W.S. 1998. Effects of interdecadal climate variability on the oceanic ecosystems of the NE Pacific. Fish. Oceanogr. **7**(1): 1–21. doi:10.1046/j.1365-2419.1998.00052.x.

Groot, C., and Margolis, L. 1991. Pacific salmon: life histories. UBC Press, Vancouver, B.C.

Hare, S.R., and Francis, R.C. 1995. Climate change and salmon production in the Northeast Pacific Ocean. *In* Climate change and northern fish populations. *Edited by* R.J. Beamish. Can. Spec. Publ. Fish. Aquat. Sci. pp. 357–372.

Hare, S.R., and Mantua, N.J. 2000. Empirical evidence for North Pacific regime shifts in 1977 and 1989. Prog. Oceanogr. **47**(2–4): 103–145. doi:10.1016/S0079-6611(00)00033-1.

Hare, S.R., Mantua, N.J., and Francis, R.C. 1999. Inverse production regimes: Alaska and West Coast Pacific salmon. Fisheries **24**(1): 6–14. doi:10.1577/1548-8446(1999)024<0006:IPR>2.0.CO;2.

Holmes, E., Ward, E., and Wills, K. 2013. MARSS: Multivariate Autoregressive State-Space Modeling. R package version 3.4.

Hurvich, C.M., and Tsai, C.-L. 1989. Regression and time series model selection in small samples. Biometrika, **76**(2): 297–307. doi:10.1093/biomet/76.2.297.

Johnson, S.P., and Schindler, D.E. 2012. Four decades of foraging history: stock-specific variation in the carbon and nitrogen stable isotope signatures of Alaskan sockeye salmon. Mar. Ecol. Prog. Ser. **460**: 155–167. doi:10.3354/meps09772.

Kalnay, E., Kanamitsu, M., Kistler, R., Collins, W., Deaven, D., Gandin, L., Iredell, M., Saha, S., White, G., Woollen, J., Zhu, Y., Chelliah, M., Ebisuzaki, W., Higgins, W., Janowiak, J., Mo, K.C., Ropelewski, C., Wang, J., Leetmaa, A., Reynolds, R., Jenne, R., and Joseph, D. 1996. The NCEP/NCAR 40-year reanalysis project. B. Am. Meteorol. Soc. **77**(3): 437–471. doi:10.1175/1520-0477(1996)077<0437:TNYRP>2.0.CO;2.

Legendre, P., and Legendre, L. 1998. Numerical ecology. Elsevier Science B.V., Amsterdam, the Netherlands.

Litzow, M.A., and Mueter, F.J. 2009. Four decades of climate-biology covariation in the Northeast Pacific: 98 updated ecosystem indicators, 1965–2006. North Pacific Research Board, Anchorage, Alaska.

Mantua, N.J., Hare, S.R., Zhang, Y., Wallace, J.M., and Francis, R.C. 1997. A Pacific interdecadal climate oscillation with impacts on salmon production. B. Am. Meteorol. Soc. **78**(6): 1069–1079. doi:10.1175/1520-0477(1997)078<1069:APICOW>2.0.CO;2.

Minchin, P.R. 1987. An evaluation of the relative robustness of techniques for ecological ordination. Vegetatio, **69**: 89–107. doi:10.1007/BF00038690.

Moss, J.H., Beauchamp, D.A., Cross, A.D., Myers, K.W., Farley, E.V., Murphy, J.M., and Helle, J.H. 2005. Evidence for size-selective mortality after the first summer of ocean growth by pink salmon. Trans. Am. Fish. Soc. **134**(5): 1313–1322. doi:10.1577/T05-054.1.

Mueter, F.J., and Norcross, B.L. 2000. Changes in species composition of the demersal fish community in nearshore waters of Kodiak Island, Alaska. Can. J. Fish. Aquat. Sci. **57**(6): 1169–1180. doi:10.1139/f00-051.

Mueter, F.J., Peterman, R.M., and Pyper, B.J. 2002. Opposite effects of ocean temperature on survival rates of 120 stocks of Pacific salmon (*Oncorhynchus* spp.) in northern and southern areas. Can. J. Fish. Aquat. Sci. **59**(3): 456–463. doi:10.1139/f02-020.

Mueter, F.J., Boldt, J.L., Megrey, B.A., and Peterman, R.M. 2007. Recruitment and survival of Northeast Pacific Ocean fish stocks: temporal trends, covariation, and regime shifts. Can. J. Fish. Aquat. Sci. **64**(6): 911–927. doi:10.1139/f07-069.

Myers, K.W., Klovach, N.V., Gritsenko, O.F., Urawa, S., and Royer, T.C. 2007. Stock-specific distributions of Asian and North American salmon in the open ocean, interannual changes, and oceanographic conditions. N. Pac. Anadr. Fish Comm. Bull. **4**: 159–177.

North, G.R., Bell, T.L., Cahalan, R.F., and Moeng, F.J. 1982. Sampling errors in the estimation of empirical orthogonal functions. Mon. Weather Rev. **110**(7): 699–706. doi:10.1175/1520-0493(1982)110<0699:SEITEO>2.0.CO;2.

Oksanen, J., Blanchet, F.G., Kindt, R., Legendre, P., O'Hara, R.B., Simpson, G.L., Solymos, P., Stevens, M.H.H., and Wagner, H. 2011. vegan: community ecology package. R package version 1.17-6.

Parker, R.R. 1962. Estimations of ocean mortality rates for Pacific salmon (*Oncorhynchus*). J. Fish. Res. Board Can. **19**(4): 561–589. doi:10.1139/f62-037.

Perry, A.L., Low, P.J., Ellis, J.R., and Reynolds, J.D. 2005. Climate change and distribution shifts in marine fishes. Science **308**(5730): 1912–1915. doi:10.1126/Science.1111322.

Peterman, R.M. 1987. Review of the components of recruitment of Pacific salmon. *In* Common strategies of anadromous and catadromous fishes. American Fisheries Society Symposium 1. *Edited by* M. Dadswell, R. Klauda, C. Moffitt, R. Saunders, R. Rulifson, and J.E. Cooper. American Fisheries Society, Bethesda, Md. pp. 417–429.

Peterman, R.M., and Wong, F.Y.C. 1984. Cross correlations between reconstructed ocean abundances of Bristol Bay and British Columbia sockeye salmon (*Oncorhynchus nerka*). Can. J. Fish. Aquat. Sci. **41**(12): 1814–1824. doi:10.1139/f84-222.

Peterman, R.M., Pyper, B.J., Lapointe, M.F., Adkison, M.D., and Walters, C.J. 1998. Patterns of covariation in survival rates of British Columbian and Alaskan sockeye salmon (*Oncorhynchus nerka*) stocks. Can. J. Fish. Aquat. Sci. **55**(11): 2503–2517. doi:10.1139/f98-179.

Portman, D.A., and Gutzler, D.S. 1996. Explosive volcanic eruptions, the El Niño–Southern Oscillation, and U. S. climate variability. J. Clim. **9**(1): 17–33. doi:10.1175/1520-0442(1996)009<0017:eveten>2.0.co;2.

Pyper, B.J., and Peterman, R.M. 1998. Comparison of methods to account for autocorrelation in correlation analyses of fish data. Can. J. Fish. Aquat. Sci. **55**(9): 2127–2140. doi:10.1139/f98-104.

Pyper, B.J., Mueter, F.J., Peterman, R.M., Blackbourn, D.J., and Wood, C.C. 2001. Spatial covariation in survival rates of Northeast Pacific pink salmon (*Oncorhynchus gorbuscha*). Can. J. Fish. Aquat. Sci. **58**(8): 1501–1515. doi:10.1139/f01-096.

Pyper, B.J., Mueter, F.J., Peterman, R.M., Blackbourn, D.J., and Wood, C.C. 2002. Spatial covariation in survival rates of northeast Pacific chum salmon. Trans. Am. Fish. Soc. **131**(3): 343–363. doi:10.1577/1548-8659(2002)131<0343:SCISRO>2.0.CO;2.

Pyper, B.J., Mueter, F.J., and Peterman, R.M. 2005. Across-species comparisons of spatial scales of environmental effects on survival rates of Northeast Pacific salmon. Trans. Am. Fish. Soc. **134**(1): 86–104. doi:10.1577/T04-034.1.

R Development Core Team. 2012. R: a language and environment for statistical computing [online]. R Foundation for Statistical Computing, Vienna, Austria. ISBN 3-900051-07-0. Available from http://www.R-project.org.

Roessig, J.M., Woodley, C.M., Cech, J.J., and Hansen, L.J. 2004. Effects of global climate change on marine and estuarine fishes and fisheries. Rev. Fish Biol. Fish. **14**(2): 251–275. doi:10.1007/s11160-004-6749-0.

Ruggerone, G.T., Zimmermann, M., Myers, K.W., Nielsen, J.L., and Rogers, D.E. 2003. Competition between Asian pink salmon (*Oncorhynchus gorbuscha*) and Alaskan sockeye salmon (*O. nerka*) in the North Pacific Ocean. Fish. Oceanogr. **12**(3): 209–219. doi:10.1046/J.1365-2419.2003.00239.X.

Ruggerone, G.T., Peterman, R.M., Dorner, B., and Myers, K.W. 2010. Magnitude and trends in abundance of hatchery and wild pink salmon, chum salmon, and sockeye salmon in the North Pacific Ocean. Mar. Coast. Fish. Dynam. Man. Ecosyst. Sci. **2**: 306–328. doi:10.1577/C09-054.1.

Schindler, D.E., Rogers, D.E., Scheuerell, M.D., and Abrey, C.A. 2005. Effects of changing climate on zooplankton and juvenile sockeye salmon growth in southwestern Alaska. Ecology, **86**(1): 198–209. doi:10.1890/03-0408.

Seo, H., Kudo, H., and Kaeriyama, M. 2011. Long-term climate-related changes in somatic growth and population dynamics of Hokkaido chum salmon. Environ. Biol. Fishes, **90**(2): 131–142. doi:10.1007/s10641-010-9725-7.

Smith, T.M., Reynolds, R.W., Peterson, T.C., and Lawrimore, J. 2008. Improvements to NOAA's historical merged land-ocean surface temperature analysis (1880–2006). J. Clim. **21**(10): 2283–2296. doi:10.1175/2007JCLI2100.1.

Tadokoro, K., Ishida, Y., Davis, N.D., Ueyanagi, S., and Sugimoto, T. 1996. Change in chum salmon (*Oncorhynchus keta*) stomach contents associated with fluctuation of pink salmon (*O. gorbuscha*) abundance in the central subarctic Pacific and Bering Sea. Fish. Oceanogr. **5**(2): 89–99. doi:10.1111/j.1365-2419.1996.tb00108.x.

Thomson, R.E., and Gower, J.F.R. 1998. A basin-scale oceanic instability event in the Gulf of Alaska. J. Geophys. Res. **103**(C2): 3033–3040. doi:10.1029/97JC03220.

Wolter, K., and Timlin, M.S. 1998. Measuring the strength of ENSO events: How does 1997/98 rank? Weather, **53**: 315–324. doi:10.1002/j.1477-8696.1998.tb06408.x.

Zuur, A.F., and Pierce, G.J. 2004. Common trends in northeast Atlantic squid time series. J. Sea Res. **52**: 57–72. doi:10.1016/j.seares.2003.08.008.

Zuur, A.F., Fryer, R.J., Jolliffe, I.T., Dekker, R., and Beukema, J.J. 2003*a*. Estimating common trends in multivariate time series using dynamic factor analysis. Environmetrics, **14**: 665–685. doi:10.1002/env.611.

Zuur, A.F., Tuck, I.D., and Bailey, N. 2003*b*. Dynamic factor analysis to estimate common trends in fisheries time series. Can. J. Fish. Aquat. Sci. **60**(5): 542–552. doi:10.1139/f03-030.